Institut für Lebensmittelsicherheit und -hygiene
der Vetsuisse-Fakultät Universität Zürich

Direktor: Prof. Dr. Dr. h.c. Roger Stephan

Arbeit unter wissenschaftlicher Betreuung von
PD Dr. Taurai Tasara

Comparative phenome and genome analysis of two clonally identical *Listeria monocytogenes* strains that were recovered five years apart from a persistent human prosthetic hip joint infection

Inaugural-Dissertation

zur Erlangung der Doktorwürde der
Vetsuisse-Fakultät Universität Zürich

vorgelegt von

Francis Muchaamba

Tierarzt
von Harare, Zimbabwe

genehmigt auf Antrag von

Prof. Dr. Dr. h.c. Roger Stephan, Referent

Prof. Dr. Franz Allerberger, Korreferent

2018

Contents

Abstract

We isolated two clonally identical *L. monocytogene*s strains five years apart from a persistent human prosthetic hip joint infection (PJI). N843-15 (2015 isolate), grew slower, aggregated during growth in broth and was impaired in motility compared to N843-10 (2010 isolate). Microscopy revealed filamentation and morphological defects consistent with incomplete cell division and disrupted cell wall synthesis in N843-15. On phenotypic microarrays N843-15 showed diminished carbon source utilization and stress tolerance capacities in comparison to N843-10. N843-15 also showed higher antibiotic sensitivity and produced less biofilm than N843-10. Furthermore, N843-15 had lower cell invasion but similar hemolysis capacity compared to N843-10. Both strains were significantly diminished in hemolysis, cell invasion and zebrafish virulence when compared to other *L. monocytogenes* strains. Genome analysis uncovered 26 SNPs and 44 InDels within the N843-15 genome compared to N843-10. Mutations in N843-15 *rnjA*, *htrA*, and *lmo2812* genes, might explain the main phenotypic alterations detected in this strain. Consistent with their low virulence capacity, both strains carry an identical mutation in the *prfA* gene leading to a truncated virulence regulator PrfA protein. Overall our findings provide insights into molecular mechanisms associated with adaptation and evolution of *L. monocytogenes* within the PJI environment.

Keywords: *Listeria monocytogenes*, prosthetic joint infection, phenotype, genome

Zusammenfassung

Zwei *L. monocytogene*s Stämme wurden im Abstand von fünf Jahren im Zusammenhang mit einer persistenten prostethischen Hüftgelenksinfektion (PHGI) bei einem Menschen isoliert. Obwohl die beiden Stämme clonal identisch waren, wiesen sie signifikante phänotypische und genotypische Unterschiede auf. N843-15 wuchs langsamer, bildete Aggregate und wies im Vergleich zu N843-10 eine verminderte Beweglichkeit auf. N843-15 zeigte einen filamentierten Phänotyp und morphologische Defekte, die auf eine unvollständige Zellteilung und eine unterbrochene Zellwandsynthese hindeuten. Beide Stämme wiesen im Vergleich zu *L. monocytogenes* Referenzstämmen eine signifikant verringerte Hämolyse, Invasivität und Virulenz im Zebrafischmodell auf. Ein Vergleich der Genome beider Stämme zeigte, dass im N843-15 Genom 26 SNPs und 44 InDels vorhanden waren. Die Unterschiede umfassten auch drei Pseudogene, *rnjA*, *htrA*, und *lmo2812*, die zum Phänotyp des Stammes beitragen könnten. Beide Stämme wiesen zudem eine Deletion eines einzelnen Nukleotids auf, die zu eine Trunkierung von *prfA* führt, welche mit der verminderten Virulenz beider Stämme im Einklang steht. Insgesamt unterlegen diese Resultate die phänotypischen Abweichungen zwischen diesen beiden Stämmen und können zudem Einblicke in molekulare Mechanismen gewähren, die zu einer langfristigen Adaptation und Evolution von *L. monocytogenes* bei prosthetischen Gelenksinfektionen beitragen.

Schlüsselwörter: *Listeria monocytogenes*, prosthetische Gelenksinfektion, Phänotyp, Genom

Introduction

Listeriosis caused by *Listeria monocytogenes* is a serious food borne disease, predominantly affecting neonates, pregnant women, elderly and immunocompromised individuals with high mortality rates in these groups (Anonymous, 2017; Anonymous, 2018; Radoshevich and Cossart, 2018). In the risk group, such infections commonly manifest as life-threatening meningitis, bacteremia, and feto-maternal complications (Allerberger and Wagner, 2010; Anonymous, 2017; Radoshevich and Cossart, 2018). Listeriosis may however also present as self-limiting gastrointestinal illness in immunocompetent hosts. Though rare, focal infections with *L. monocytogenes* affecting various organs including bone and joint have also been described (Allerberger and Wagner, 2010; Del Pozo *et al*., 2013).

L. monocytogenes septic arthritis is an infrequent manifestation of listeriosis with relatively few cases described in the literature to date (Charlier *et al*., 2012, Chavada *et al*. 2014; Bader *et al*., 2016). On the other hand, most described cases of osteoarticular *Listeria* infections involve orthopedic implant devices, predominantly joint arthroplasties, which has led to suggestions that the presence of prosthesis might increase the likelihood of articular *Listeria* infection (Cone *et al*., 2001; Chougle and Narayanaswamy, 2004; Kesteman *et al*., 2007; Charlier *et al*., 2012; Bader *et al*., 2016). In addition to the presence of implants, osteoarticular listeriosis is more common in individuals who are above 60 years, immunosuppressed or undergoing corticosteroid therapy, having underlying neoplasia, and or diabetes (Del Pozo *et al*., 2013; Bush *et al*., 2015; Bader *et al*., 2016). Rheumatoid arthritis has been seen to carry the greatest risk of septic arthritis, probably as a consequence of frequent joint prosthetic implants and intraarticular and systemic immunosuppressive therapies in these patients (Kleemann *et al*., 2009; Charlier *et al*., 2012).

Though *L. monocytogenes* is not the main bacterium involved in prosthetic joint infection (PJI) or periprosthetic joint infections, reports of such infections are on the rise probably due to the upsurge in prosthetic joint replacements in listeriosis high-risk groups (Charlier *et al*., 2012; Bush *et al*., 2015; Bader *et al*., 2016). These infections are associated with substantial morbidity, impaired joint function, and at times limb amputation (Bush *et al*., 2015). On the basis of the onset of symptoms after implantation, PJI can be classified as early (occurring in 3 months or less), delayed (occurring in 3 to 24 months), and late (occurring more than 24 months) after arthroplasty (Shuman *et al*., 2012; Bush *et al*., 2015).

No specific treatment protocol is in place for the treatment of osteoarticular listeriosis. Several antibiotic treatment regimens and durations have been reported, with ampicillin or amoxicillin, either alone or in combination with gentamicin being the most commonly used antibiotics (Allerberger and Wagner, 2010; Charlier *et al*., 2012; Bush *et al*., 2015). The duration of treatment ranges from two weeks to one and a half years with some patients being placed on life-long oral antibiosis (Charlier *et al*., 2012; Bush *et al*., 2015). Treatment failures are relatively high for *Listeria* PJI cases who receive antibiotic therapy alone without surgical removal of the infected prosthesis (Charlier *et al*., 2012; Bush *et al*., 2015; Bader *et al*., 2016). As such combining antibiotic therapy and replacement of the infected joint prosthesis seems to have the best prognosis in these cases (Charlier *et al*., 2012; Bader *et al*., 2016).

Predictive models suggest that cases of osteoarticular listeriosis may become more common as the size of the population having specific risk factors related to this condition increases. To further narrow the knowledge gap in this area, we aimed to understand the basis of a specific case we encountered from our routine diagnostic laboratory services. Two *L. monocytogenes* strains were isolated from an 84-year-old female's prosthetic hip joint, the first strain at the beginning of the infection and the second strain five years later from a chronic infection. On both occasions the listeriosis clinically presented as a fistula affecting her left lateral hip. Surprisingly the patient and bacterium seemed to have been in a symbiotic relationship, as the patient had harbored this infection with little to no deleterious health effects on herself. The patient also suffered from chronic obstructive pulmonary disease (COPD), for which she received several antibiotic treatments during this period.

Since these two strains, belonging to the same clonal complex, upon preliminary examination differed phenotypically, we used different phenome and genome-based approaches in order to investigate possible physiological and molecular adaptive changes that may have evolved in the original clone leading to these two phenotypically differing strains during long-term exposure to the prosthetic human hip joint environment.

Methods and Materials

Bacterial strains. Strains used in this study are listed in Table 1. *Listeria monocytogenes* strains N843-10 (isolated in 2010) and N843-15 (isolated in 2015), isolated five years apart from the same chronic prosthetic human hip joint capsule infection were studied. Where necessary the *L. monocytogenes* strains LL195, EGDe, N12-1273 as well as *Listeria innocua* JF5051 were used as references. Cultures were stored at -80 °C in brain heart infusion medium (BHI) supplemented with 20% glycerol. Strains were initially grown on blood agar or BHI agar plates at 37°C for 16 hours to give single colonies, and then pre-cultured twice in BHI broth (37°C, 150 rpm) for 16 hours, to get stationary phase secondary cultures. Cultures from the second BHI pre-culture were subsequently used in experiments unless otherwise stated. All experiments were carried out in triplicates unless otherwise stated.

TABLE. 1. Strains used in this study

Strain ID	Description	References
EGDe	Rabbit isolate and reference strain, serotype 1/2a, CC9	Glaser *et al.*, 2001
N843-10	2010 patient PJI isolate, serotype 1/2a, CC412	This study
N843-15	2015 patient PJI isolate, serotype 1/2a, CC412	This study
N12-1273	Sporadic human listeriosis isolate, serotype 1/2a, CC412	Althaus *et al.*, 2014
LL195	1983 Swiss listeriosis outbreak, serotype 4b, CC1	Bille, 1990
J5051	*Listeria innocua* used as a negative control	Guldimann *et al.*, 2015
N11-1850	2011 milk isolate, serotype 4b, CC217, used as positive control in biofilm assays	Ebner *et al.*, 2015

Quantification of cell growth. A BHI secondary pre-culture from each strain standardized to an optical density (OD_{600}) of 1.0 was diluted 1:100 in 10 ml BHI and incubated at 37°C and 150 rpm. Growth was monitored after 0, 2, 4, 6, 8, 10, 12 and 24 hours by plating out 10-fold serial dilutions on BHI agar and OD_{600} measurement. Experiments were repeated 3 times and runs were done in duplicates. The means and standard deviations were calculated based on the biological triplicates.

Multilocus sequence typing (MLST) and serotyping. MLST was performed based on seven housekeeping gene fragments as previously described (Stessl *et al*., 2014; Moura *et al*., 2016) using the amplification and sequencing primers that are described on the Institut Pasteur website (http://bigsdb.web.pasteur.fr/listeria/listeria.html). Sequences for each gene fragment were assembled from at least two independent PCR products and trimmed to a constant length as indicated on the website. PCR-serogroup were deduced in silico from whole genomic sequences using the BIGSdb platform for each of the isolates (Jolley and Maiden, 2010; Moura *et al*., 2016). The isolates were serotyped with Listeria O and H antisera (Listeria Antisera set, Denka Seiken co., Ltd, Japan), according to the manufacturer's recommendations.

Light microscopy. For visualization of bacterial cells, 100 μl of overnight cultures grown in BHI broth, were fixed onto objective slides, Gram stained and processed for microscopic analysis. Slides were examined and photographed with a Leica DM4000B digital microscope through a 100x/1.3 oil-immersion objective.

Electron microscopy of thin sections. For electron microscopy, cells were harvested from overnight BHI cultures by centrifugation (6 000 g at 25°C for 5 min). Then the pellets were fixed with 2.5% glutaraldehyde (Electron Microscopy Sciences) buffered in 0.1 M Sodium phosphate buffer (Sigma, Buchs, Switzerland) for 2 hours at room temperature, then washed 3 times with 0.1 M sodium phosphate buffer, fixed, and stained with 1% osmium tetroxide (Sigma, Buchs, Switzerland). The samples were dehydrated in ascending concentrations of ethanol followed by dehydration with propylene oxide (Sigma, Buchs, Switzerland) and infiltration in 30% and 50% Epon (Epoxy embedding medium, Sigma, Buchs, Switzerland). From each pellet, 0.9 mm toluidine blue stained semi thin sections were produced. Representative areas were trimmed and subsequently 90 nm, lead citrate (Merck, Germany) and uranyl acetate (Serva Electrophoresis, Baden-Würtenberg, Germany) contrasted ultrathin sections were produced and viewed under a transmission electron microscope (TEM Phillips CM10) in the Institute for Veterinary Pathology, Zuerich, (IVPZ) at the University of Zurich.

Motility assay. 5 μl of overnight BHI culture of the different strains was spot inoculated on the surface of soft BHI agar (0.25% agar) plates containing 0.05% Triphenyltetrazolium Chloride (TTC) and incubated at 37°C and 25°C respectively for 48 hours. Motility was determined by measuring the diameter of the red zone created by the spreading colony. The

principle of this test is that, as the microbes grow, they incorporate and reduce TTC creating a diffuse red color which is much easier to visualize and measure.

Assessing the ability of supernatants from other Listeria strains on N843-15 aggregation during growth. The effects of supernatants from N843-10 and EGDe strains on N843-15 growth characteristics was investigated following procedures previous described with few modifications (Alonzo *et al*., 2011). Briefly, supernatants from EGDe, N843-10 and N843-15 cultures incubated for 2, 4, 6, 8 and 16 hours were recovered by centrifugation (10 min at 12 000 g) and sterile filtered using a 0.2 μM filter. To test for the ability of the supernatants to complement N843-15 aggregation, 100 μl of an overnight N843-15 culture was inoculated into 10 ml of the respective supernatant media collected at different time points. The supernatants were mixed with fresh BHI to cater for the nutrient loss associated with the use of supernatants derived from growing cultures according to ratios previously defined (Alonzo *et al*., 2011). The cultures were then grown at 37°C with shaking. At 8 and 16 hours the tubes were visually assessed for aggregation.

Assessing the impact of coculture with other Listeria strains on N843-15 aggregation during growth. Using BHI tubes, overnight cultures from each strain were standardized to an OD_{600} of 1.0 and diluted (1:100). Diluted EGDe or N843-10 (100 μl) were co-inoculated with N843-15 (200 μl) in the same 10 ml BHI tube. Cultures were incubated for 24 hours (37°C and 150 rpm) and then visually assessed for aggregation. To separately co-culture N843-15 and the other strains in the same tube the co-cultures were prepared as described above but N834-15 and the different strains were inoculated in compartments separated using a 2 μM pore size filter. Briefly, wells in a 24-well plate were first filled with 700 μl of a freshly inoculated (1:50 mixture) N843-15 BHI secondary culture. A 2 μM pore size filter was placed on top followed by the addition of 700 μl of freshly inoculated (1:100 mixture) EGDe or N843-10 secondary cultures. Cultures were grown for 24 hours at 37°C with shaking in a Synergy HT OD reader (Biotech instruments, GmbH, Switzerland), at which point the extent of N843-15 aggregation was visually assessed.

Antibiotic sensitivity. Prior to each experiment, bacteria were plated by streaking on blood agar plates and grown overnight at 37°C. Tests for antibiotic susceptibility using commercial E test strips against a panel of 8 antimicrobials: amoxicillin and clavulanic acid (Amoxy Clav),

cephalothin, tetracycline, ciprofloxacin, penicillin G, sulfamethoxazole, azithromycin and gentamicin, were done in accordance with the manufacturers recommendations. Briefly bacteria solutions of 0.5 McFadden standard density were plated to form a lawn on the surface of a Muller Hinton plus blood agar plate. An appropriate antibiotic E test strip was then placed on respective plates and results were assessed after 48h of incubation at 37°C. The minimum inhibitory concentration (MIC) was defined as the highest concentration at which the colonies touched the E test strip.

Biofilm assays. Biofilm experiments were performed in Tryptone soy broth (TSB) medium at 37°C. Overnight aliquot of TSB secondary cultures (1:40) were added to fresh TSB medium then 100 μl of this mixture was added to 96-well microtiter plates. Biofilms were grown for 96 hours at 37°C. Unbound cells were removed by washing 3 times with 150 μl sterile deionized water then inversion and tapping on absorbent paper. Microplates were dried at 37°C for 30 mins, and adherent cells stained with 150 μl aqueous crystal violet for 20 minutes. Excess stain was removed by 5 washings with deionized water. Then bound cells were quantified by addition of 96% ethanol, and dissolved crystal violet was measured at an optical density of 595 nm using a Synergy HT OD reader (Biotech instruments, GmbH, Switzerland). Each biomass was standardized relative to *L. monocytogenes* N11-1850.

Hemolysis Assays. For hemolysis analysis, sterile filtered 1M dithiothreitol (DTT) (Sigma Aldrich) treated supernatant collected from early stationary phase cultures were used. These were collected from cultures grown using overnight cultures to make 1:100 dilutions in pre-heated BHI (1:20 for N843-15) and incubated at 37°C for 5 hours. The cultures were first standardized to the same optical density using BHI and centrifuged to collect the supernatants. To activate the hemolysin, a 1:200 dilution of 1M DTT and each of the supernatant was made and incubated for 1 hour at 37°C. 100 μl of a 2% washed human red blood cells PBS solution was pipetted to respective 96 well plate wells. Then 100 μl of the DTT activated supernatant was added. The bacterial supernatant and RBC mixture was incubated at 37°C for 40 mins to allow hemolysis to occur. After which it was centrifuged for 5 min at 3100 g and then 100 μl of each lysate was transfer to a new 96 well plate. The degree of hemolysis was assessed by measuring absorbance of the lysate at 420 nm using the Synergy HT OD reader (Biotech instruments, GmbH, Switzerland). All experiments were carried out in triplicate and the

internal control strains *L. monocytogenes* LL195, N12-1273 and *L. innocua* JF5051 were included.

Cell Invasion assays. Cell invasion assays were performed in the human enterocyte-like Caco-2 (ATCC® HTB-37™) cell line. Cells were grown to confluence in a 96-well plate overnight at 37°C, 5% CO_2 in Eagle's minimum essential medium (MEM), (Life technologies, Switzerland) supplemented with 20% fetal bovine serum. The monolayers were washed with pre-warmed PBS (37°C) and then infected with *L. monocytogenes* strains at a multiplicity of infection (MOI) of 0.01 in MEM. Following 30 mins of incubation the medium was removed, then cells were washed with PBS and overlaid with MEM medium containing 0.01 mg/ml gentamicin and incubated for another 60 mins at 37°C to kill extracellular bacteria. At the end of the incubation the cells were washed five times with 100 μl warm PBS and 100 μl of 40 mg/ml saponin was added to lyse the cells. The lysate was serially diluted and cell count was done to determine the number of *L monocytogenes* recovered in comparison to the number used to infect the Caco-2 cells. All experiments were carried out in triplicate and included the reference strain *L. monocytogenes* LL195 and *L. innocua* JF5051 as a negative control.

Zebra fish microinjection assays. Zebrafish husbandry and assays were performed as previous described (Eshwar *et al*., 2017) with a few modifications. The *Danio rerio wik* zebrafish line strains were used in this study. All experiments were performed with the approval (no. 216/2012) from the Veterinary Office, Public Health Department, Canton of Zurich (Switzerland). Bacteria for microinjection experiments were harvested from stationary phase BHI bacteria cultures by centrifugation and washing with DPBS, then standardized to the same CFU through plate counts and appropriate dilutions. Two-day post fertilization embryos were injected with approximately 500 CFU in 1–2 nl volume of a bacterial suspension in DPBS into the blood circulation via the caudal vein. The number of CFU injected was determined by direct microinjection of a DPBS droplet on agar plates and confirmed by disintegrating five embryos individually immediately after microinjection and plating the lysates on BHI agar. Post infection embryos were placed into 24-well plates (one embryo per well) in 1 ml E3 medium per well, incubated at 28°C and observed for signs of disease and survival under a stereomicroscope twice a day. The number of dead larvae was determined visually based on the absence of a heartbeat.

Phenotype microarray. The metabolic and stress tolerance profiles of the strains was measured using Biolog Phenotype Microarrays (PM). We analyzed carbon source utilization (PM01 and PM02) as well as resistance to osmotic and pH stress (PM09 and PM10) phenotypic profiles. The full list of the tested compounds can be obtained from http://www.biolog.com/pdf/pm_lit/PM1-PM10.pdf. Prior to PM experiments, bacteria from glycerol stocks stored at -80°C were grown overnight at 37°C on BHI agar. PM experiments were performed following standard Biolog Inc. protocols with a few modifications. Briefly, single colonies of the bacteria grown on BHI agar was sub-cultured on BHI agar plates and incubated overnight at 37°C. A 81% transmittance cell suspension in Biolog solution IF-0a was then prepared by re-suspending the bacteria grown on BHI agar plates. This suspension was then diluted with Biolog additive solution for the specific plate at manufacturers prescribed ratio. 100 μl of the final cell suspension was then transferred to each well of respective PM plates. The plates were incubated at 37°C with bacterial growth being read every 15 mins using Biolog reader for 24 hours. Each experiment was performed in duplicate.

Genome analysis. Genomic DNA was isolated from the strains N843-10 and N843-15 using the GenElute Bacterial Genomic DNA Kit (Sigma, Buchs, Switzerland) and sequenced at the ChunLab at Seoul National University using the Pacific Biosciences single-molecule real-time sequencing technology (SMRT). Genome sequences were assembled de novo using the SMRT Analysis 2.3.0 software. Genomes were annotated and compared using the Rapid Annotation using Subsystem Technology (RAST) and Seed Viewer (http:// rast.nmp-dr.org/). A Dot-Plot analysis of the genomes was performed using Gepard (Krumsiek *et al*., 2007). MAUVE was used to align the genomes and to derive the coordinates for the positions of the single nucleotide polymorphisms (SNPs), insertions and deletions (InDels) (Darling *et al*., 2010). Genes of interest were searched and compared between the genomes using CLC genomics Workbench (Qiagen, Prismet, Denmark) and by BLASTn and BLASTp using the National Center for Biotechnology Information (NCBI) platform (blast.ncbi.nlm.nih.gov/Blast.cgi). Genomes were compared in correlation with PM data using the DuctApe software (Galardini *et al*., 2014) to detect genes encoding enzymes that cloud be involved in the metabolic pathways responsible for the phenotypes observed with regard to carbon source utilization on PM01 and PM02. But only genes described in the Kyoto Encyclopedia of Genes and Genomes (KEGG) database were considered in this approach.

Statistical analyses. All experiments presented were performed independently at least three times unless stated otherwise. JMP software (Version 12.1.0, SAS Institute Inc., NC, USA) was used for statistical analysis of data. One-way ANOVA with post-hoc Tukey HSD tests were used to assess statistical significance of differences relative to the reference strains as well as between the strains N843-10 and N843-15. P values of < 0.05 were considered to be statistically significant. For PM data analysis DuctApe and opm version 1.3.64 software's were used as previously described (Galardini *et al*., 2014; Göker *et al*., 2016). Briefly, for opm based analysis the reference parameter was area under the curve. Whilst for DuctApe the parameter, activity index (AV), was calculated to rank kinetic curves, providing information about the ability to be active under a specific culture condition. The AV parameter was obtained through k-means clustering on maximum growth, area, average height, lag time and slope. For each compound tested, the final result was expressed as the mean of two replicates. The bacterium was not able to respire under conditions were AV value was equal to zero, whilst it was able to respire under conditions were the AV values were higher than zero.

Result

***L. monocytogenes* strains N843-10 and N843-15 are clonally identical but differ in growth, aggregation and swarming motility.** *L. monocytogenes* strains N843-10 and N843-15 that were isolated in 2010 and 2015, respectively, from the same prosthetic hip joint listeriosis infection were compared with respect to growth and swarming motility phenotypes. Compared to N843-10, N843-15 grew significantly slower on blood agar plates as well as in BHI broth cultures (Figs. 1A and 1B). Moreover, during growth in BHI broth in a shaking incubator, N843-15 formed aggregates and eventually sedimented whilst N843-10 did not (Fig. 1C). In addition, while N843-10 formed a tight pellet after centrifugation, the pellet formed by N843-15 was loose and fluffy (data not shown). Swarming motility comparison on semi-solid BHI agar at 25°C showed that motility in N843-15 was significantly diminished compared to N843-10 (Fig. 1D).

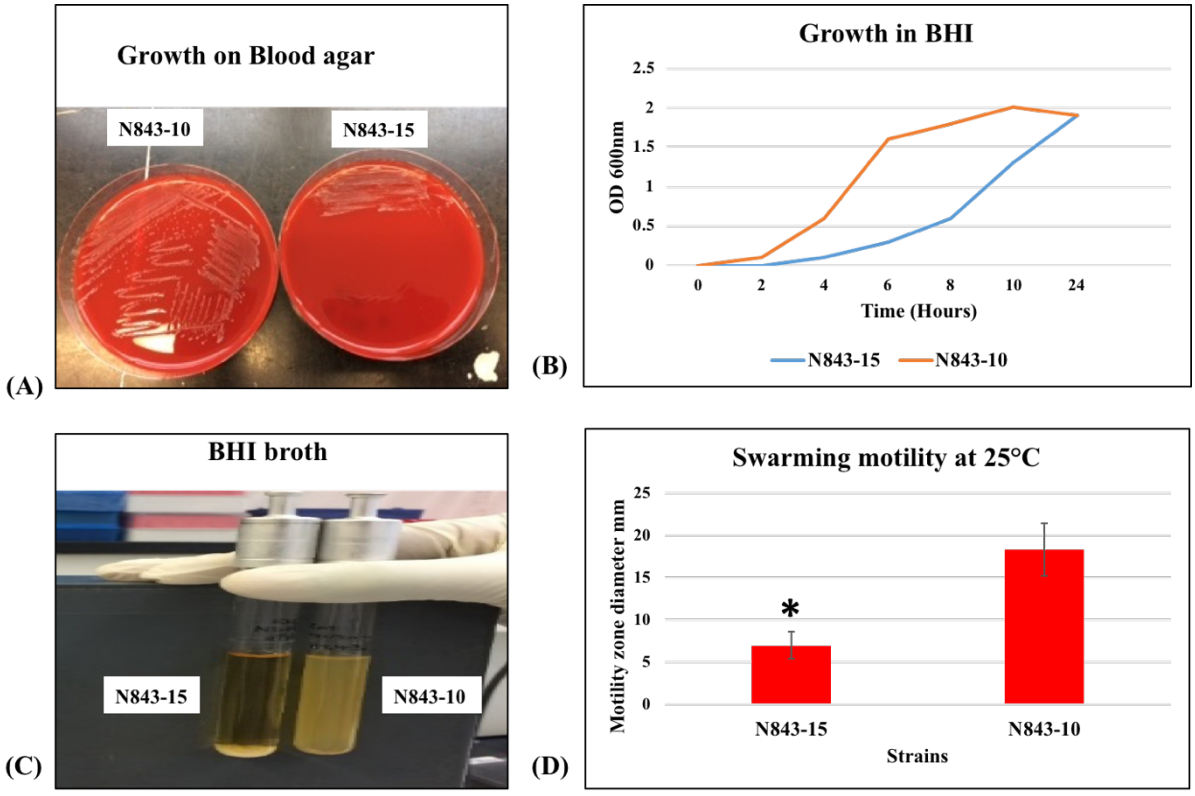

FIG. 1. N843-15 exhibits slower growth, atypical aggregation behavior and reduced motility. **(A)** N843-15 displays slower growth compared to N843-10 on blood agar. **(B)** N843-15 grows slower compared to N843-10 in BHI broth. **(C)** N843-15 aggregated and eventually sedimented whereas the N843-10 did not upon growth in BHI broth. **(D)** N843-15 has reduced swarming motility compared to N843-10. Swarming motility was assessed by spotting 5 μl of each strain on semi-solid BHI-TTC agar and measuring the colony growth diameter after 48 hours of incubation at 25°C. Results presented are the means and standard deviations from three independent experiments. * Indicates significantly lower motility zone diameter in N843-15 compared to N843-10 ($P < 0.05$).

As these two isolates from the same infection differed phenotypically we wondered if they were genetically different. To ascertain their ancestry, we used MLST and serotyping. PCR serotyping classified both isolates as PCR serotype 1/2a. MLST typing revealed that N843-10 and N843-15 were both ST412 and belonged to clonal complex 412 (CC412).

L. monocytogenes **N843-15 displays major defects in cell morphology compared to N843-10.** Next, microscopic examination was undertaken in order to further investigate the growth and aggregation phenotypic differences displayed between the N843-10 and N843-15 strains. Gram stained N843-15 cells comprised mostly of long filamented chains suggesting some form of cell division defects in this strain, whilst in contrast, N843-10 cells showed typical *L. monocytogenes* cell morphology comprising largely of single rods and short chains (Fig. 2A).

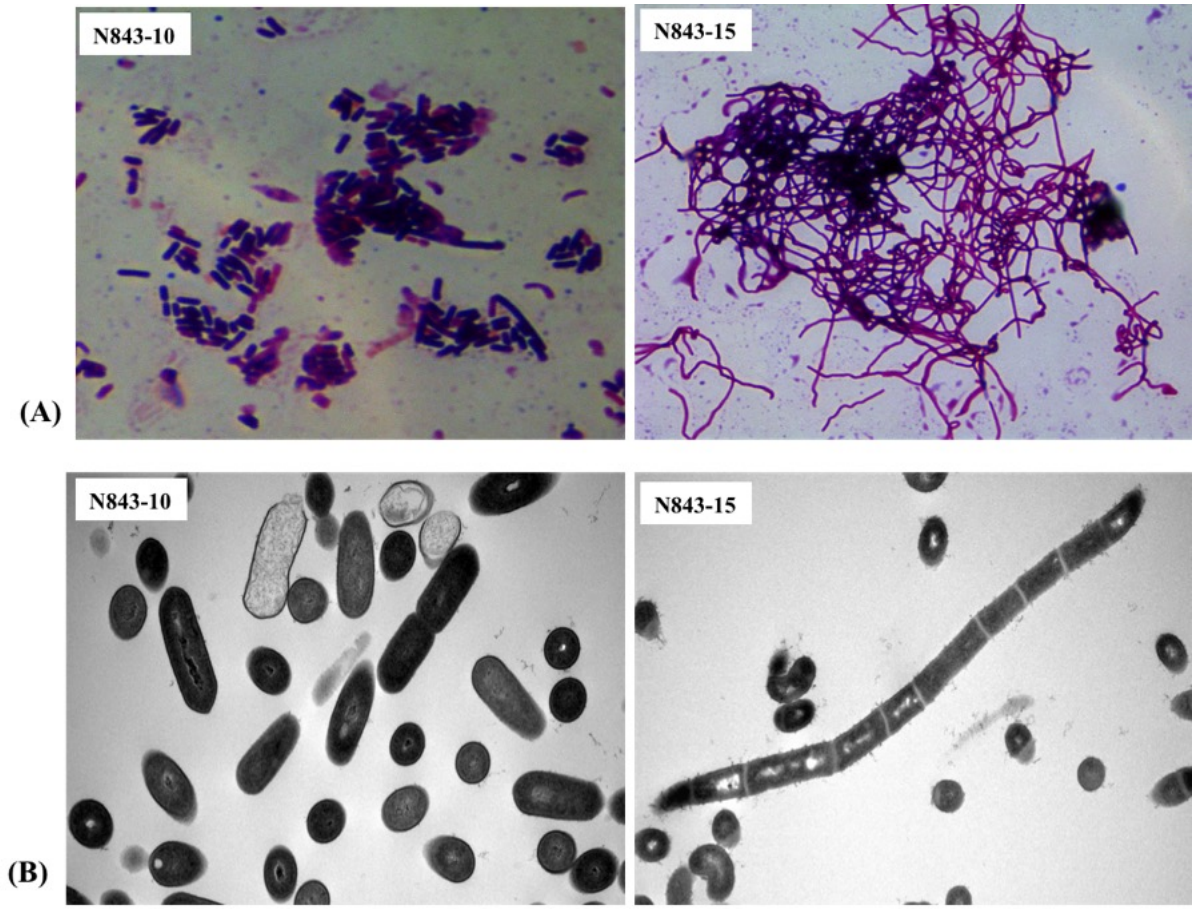

FIG. 2. N843-10 and N843-15 cells show major morphological differences. **(A)** N843-10 retains the typical *L monocytogenes* morphology of single rods and short chains whilst N843-15 is highly filamentous under the light microscope. **(B)** Electron microscopy (EM) images showing that the filamented phenotype in N843-15 is due to chains of unseparated cells whereas N843-10 showed typical *L. monocytogenes* morphology of single rods and short chains.

Besides confirming the filamented chain phenotype in N843-15, electron microscopic examination further indicated cell division defects related to cell septum formation and separation in N843-15 (Fig. 3). In contrast to N834-10, cells of N843-15 appeared highly irregular and were arranged in long chains with varying length and lacked a well-defined structure. N843-15 also has a disordered peptidoglycan layer with loosely attached fragments of peptidoglycan projecting from its surface giving it a solar flare appearance compared to the well-organized peptidoglycan of the wild-type strain N843-10 (Fig. 3).

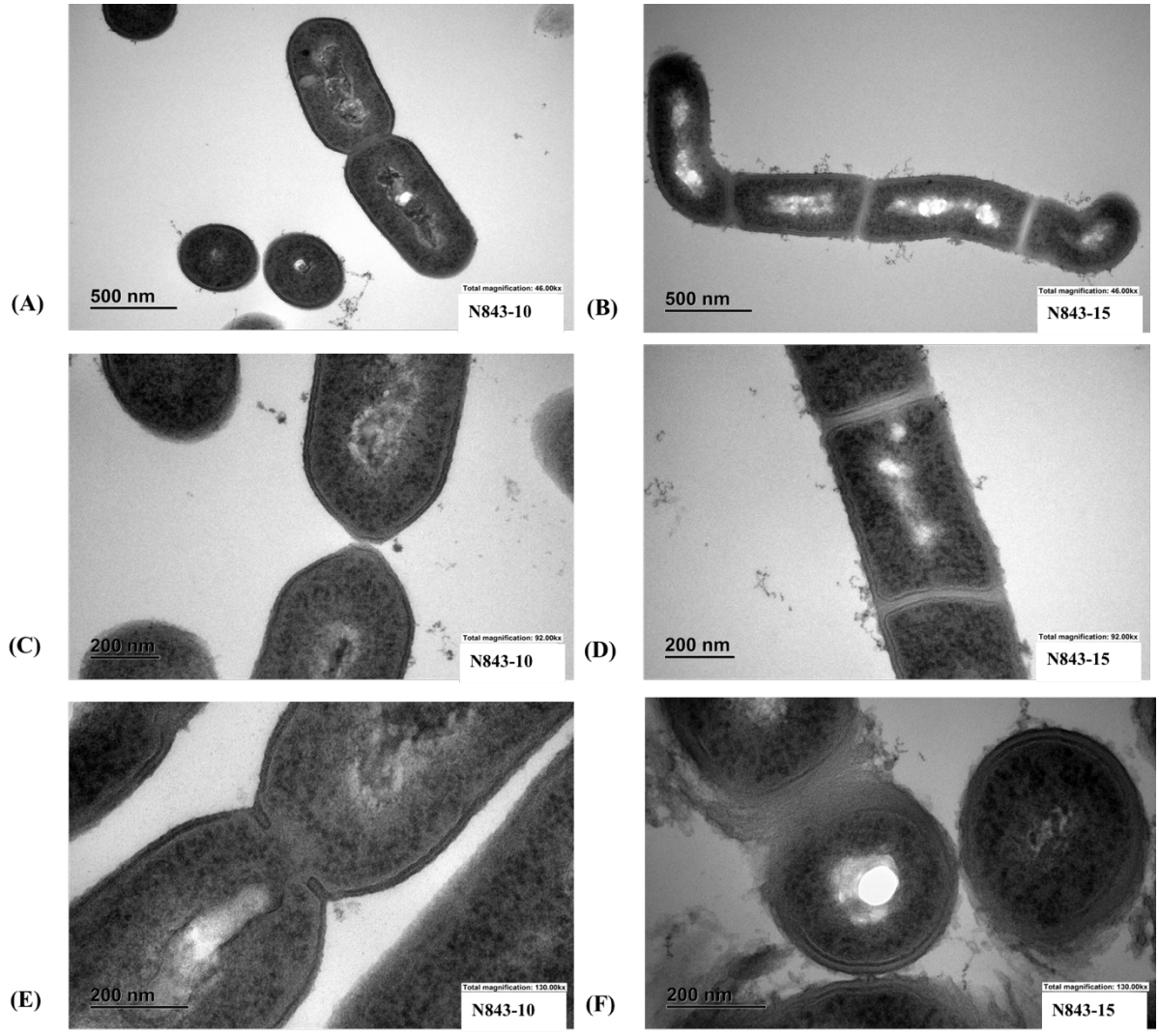

FIG. 3. EM reveals variations between N843-10 and N843-15 cell morphology. **(A)**. N843-10 displays typical *L. monocytogenes* morphology of rod shaped cells whereas the filamented N843-15 cells have variable shape **(B)** N843-10 cells displaying normal cell wall morphology and separation during cell division whilst N843-15 cells displaying altered cell wall morphology and lacks clear cell division septum demarcation. **(C)** N843-10 has a normal cell wall and is undergoing normal septum formation whereas N843-15 has altered cell walls with loosely attached fragments of peptidoglycan protruding from its surface giving it a solar flare appearance.

N843-15 aggregation is suppressed upon co-culturing with *L. monocytogenes* N843-10 and EGDe strains. The aggregation phenotype in N843-15 was further examined revealing that non-aggregating strains did not sediment upon addition of the N843-15 culture supernatants, whilst adding supernatants of non-aggregating strains to N843-15 cultures could not abolish aggregation of this strain (data not shown). On the other hand, co-culturing N843-15 with either N843-10 or the EGDe reference strain within the same BHI tube (data not shown) or in the same well but separated by a 2 μM pore size filter significantly reduced N843-15 aggregation (Fig. 4). These observations led us to conclude that N843-15 sedimentation might be abolished through substances that are produced during growth of N843-10 and EGDe cultures, but appear to have a very short life span. As such the aggregation during culture observed in the N843-15 could be due to such substance or substances being defective or absent in this isolate.

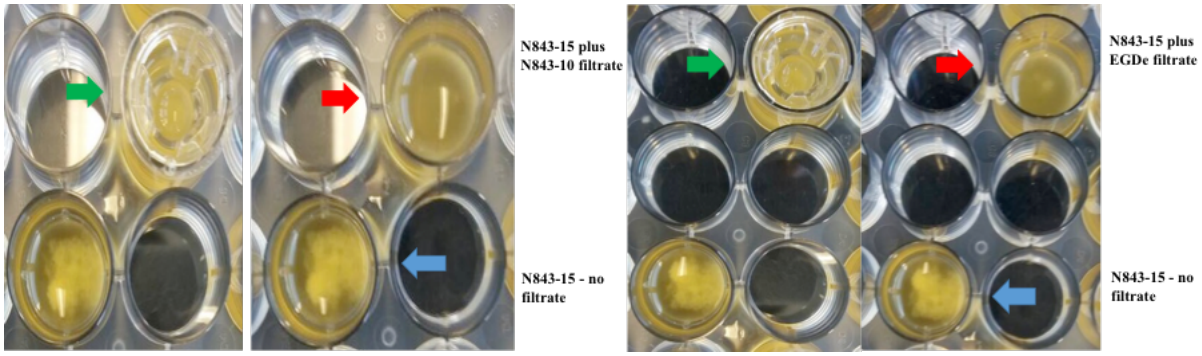

FIG. 4. Impact of coculture on N843-15 aggregation phenotype**.** N843-15 aggregation and sedimentation is reduced when co-cultured with either N843-10 or EGDe within the same well of microtiter plate but separated using a 2 μM pore size filter. Arrows indicate: green: 2 μM pore size filter in position, red: cocultured strains showing little to no sedimentation, blue: N843-15 pure culture showing aggregation.

N843-15 shows higher antibiotic sensitivity than N843-10. One possible reason for the long-term persistence of the prosthetic joint infection and emergence of N843-15 within this infected joint environment could have been a selection due to antibiotic pressure. To examine such a hypothesis the E-test based assay was used to compare the resistance levels of N843-10 and N843-15 to different antibiotics that these isolates could directly or indirectly have been exposed to during the course of their residency in the prosthetic hip joint environment. In addition, the sensitivity of the two isolates to some antibiotics commonly used in treatment of listeriosis was also compared. The minimum inhibitory concentration (MICs) determined for the different antibiotics tested showed that N843-15 was more sensitive to most of the tested antibiotics with the exception of sulfamethoxazole and gentamicin compared to N843-10 (Table. 2). It is, however, important to note that in accordance with the Clinical and Laboratory Standards Institute (CLSI) standards, both strains are considered sensitive to all the tested

antibiotics (Anonymous., 2010). As such, the persistence of the prosthetic joint listeriosis infection with *L. monocytogenes* N843 and the subsequent emergence of N843-15 to replace N843-10 within the infected joint environment could not have been due to increased antibiotic resistance in any of these two N843 strains.

TABLE. 2. MICs of different antibiotics determined for the *L. monocytogenes* N843-10 and N843-15 strains using E-tests

Antibiotic*	**MIC of N843-15 (μg/ml)**	**MIC of N843-10 (μg/ml)**	**Duration**	**Reason for treatment**
Amoxy Clav	0.10 ± 0.02	0.42 ± 0.07	10 and 6 days[1]	PJI / COPD
Cephalothin	1 ± 0	4.7 ± 1.2	1 day	Pneumonia
Azithromycin	0.29 ± 0.1	0.59 ± 0.36	3 days	COPD
Tetracycline	0.32 ± 0.1	1.33 ± 0.2	1 day	COPD
Ciprofloxacin	0.25 ± 0	0.5 ± 0	7 days	COPD
Gentamicin[2]	0.05 ± 0	0.06 ± 0.01	-	
Penicillin G[3]	0.09 ± 0	0.5 ± 0	-	
Sulfamethoxazol[4]	16 ± 0	12 ± 0	-	

∗Listed are antibiotics that the isolates could have been directly or indirectly exposed to during their residency in the joint. The antibiotics were given at different intervals in different protocols and via different routes in accordance to the physicians' recommendations. [1]Treatment given on two different occasions once for 10 days for treatment of prosthetic joint listeriosis and on another instance for treatment of Chronic Obstructive Pulmonary Disease (COPD).[2] Gentamicin was included since it is also a commonly used drug in listeriosis treatment. [3,4] These antibiotics were included in order to test the *htrA* and *rnjA* gene mutation associated hypothesis respectively.

N843-10 forms biofilms with higher biomass than N843-15. Since biofilm formation plays an important role in infections related to medical devices, we also compared N843-10 and N843-15 strains with respect to their biofilm formation efficiency. A comparison of biofilms produced at 37°C showed that N843-10 formed significantly more biofilm compared to N843-15 (Fig. 5). This suggested that the emergence and long-term survival of N843-15 in the prosthetic joint was unlikely to have been aided by an enhanced biofilm-forming ability in this strain compared to N843-10. Further N843-10 formed biofilms with no significant difference with the reference LL195 and N12-1273 a CC412 strain, whereas it was significantly less compared to a known high biofilm producing strain reference N11-1850 and thus categorizing N843-10 as a moderate biofilm producer. On the other hand, all the reference strains formed significantly more biofilm compared to N843-15 categorizing this strain as a low biofilm producer.

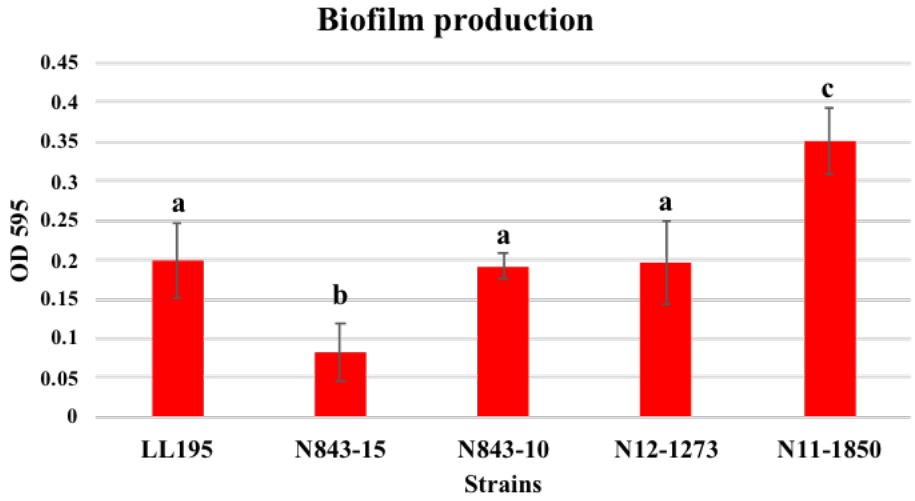

FIG. 5. N843-10 shows higher biofilm forming capacity than N843-15. Data showing the means and standard deviations of three independent biological experiments are presented. Bars that share a letter are not significantly different, whereas those marked with different letters are significantly different compared to each other ($P < 0.05$ based on one-way ANOVA and Tukey post-hoc test pairwise comparison of all the strains).

Virulence comparison of N843-10 and N843-15. The two PJI isolates were next evaluated with respect to their virulence capacity. Both strains displayed similar levels of hemolysis on human red blood cells. These levels, although above those of the *L. innocua* negative control, were significantly less in comparison to the 1983 Swiss listeriosis outbreak strain LL195, as well as compared to another CC412 strain, N12-1273, which was isolated from a sporadic human listeriosis case (Fig. 6A). Meanwhile a comparison of the two strains with respect to cell invasion capacity in the Caco-2 epithelial cell infection model showed significantly lower cell invasion ability in N843-15 compared to N843-10 (Fig. 6B). Both strains were, however, also significantly less invasive compared to LL195 used as a reference strain. In the zebrafish embryo based multicellular infection model both N843-10 and N843-15 strains were found to be avirulent. In zebrafish embryos infected using the blood stream injection route, both N843-15 and N843-10 were unable to induce any clinical signs or mortality 72 hours post infection, whereas the reference strains LL195 had induced 100% and N12-1273 had induced 50% mortality of the zebrafish embryos within 24 and 72 hours of infection, respectively (data not shown).

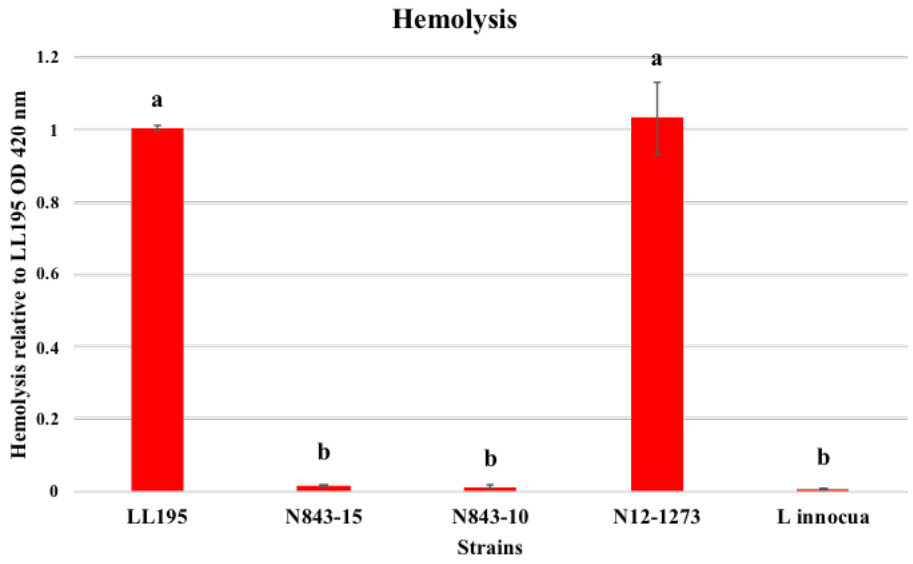

A

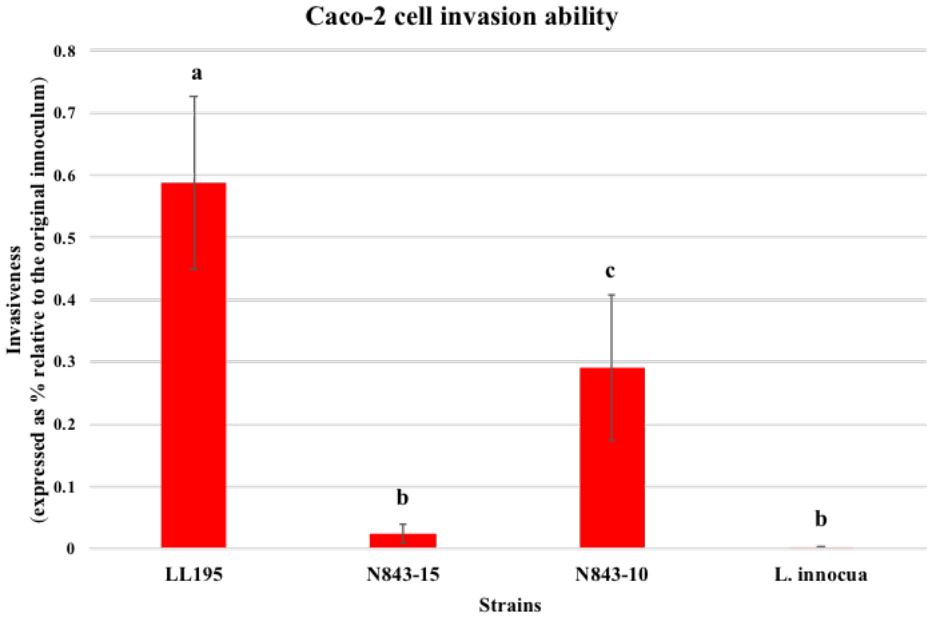

B

FIG. 6. Comparison of hemolysis and Caco-2 cell invasion capacities. **(A)** N843-10 and N843-15 are poorly hemolytic compared to *L. monocytogenes* strains LL195 and N12-1273 (**B**) N843-15 showed lower cell invasion capacity compared to N843-10, however, both strains are significantly less invasive in comparison to the reference strain LL195. Data showing the means and standard deviations of three independent biological experiments are presented. Bars that share a letter are not significantly different, whereas those marked with different letters are significantly different compared to each other ($P < 0.05$ based on one-way ANOVA and Tukey post-hoc test pairwise comparison of all the strains).

Phenotypic microarray-based comparison of N843-10 and N843-15. In order to further investigate phenotypic differences that exist between N843-10 and N843-15 strains, Biolog phenotypic microarrays were also used. N843-15 showed a narrow carbon source utilization profile as well as altered osmotic and pH stress tolerance capacities compared to N843-10, (Fig. 7, Table. 3). Overall N843-15 showed generally slower metabolic rate compared to N843-

10 on most of the carbon sources, pH and osmotic stress conditions tested (data not shown). Growth evaluation on different carbon sources on PM01 and PM02 revealed that N843-15 utilized 29 whilst N843-10 utilized 42 of the 190 tested carbon sources (Fig. 7B). N843-10 was able to utilize all the 29 carbon sources which were also utilized by N843-15 (data not shown). Notably among the 13 carbon sources utilized by N843-10 but not N843-15, there were some intracellular relevant carbon sources such as glycerol, maltose and cellobiose as well as food relevant carbon sources such as pectin and D-tagatose (Table. 3). Meanwhile growth analysis on PM09 showed that the N843-15 strain had reduced tolerance to 12 osmotic stress conditions including sodium chloride, sodium nitrite, sodium benzoate and sodium lactate when compared to N843-10. Interestingly under pH stress conditions on PM10, the N843-15 strain was found more tolerant to alkaline conditions compared to N843-10 in presence of β-Phenylethylamine at pH 9.5 (Table. 3).

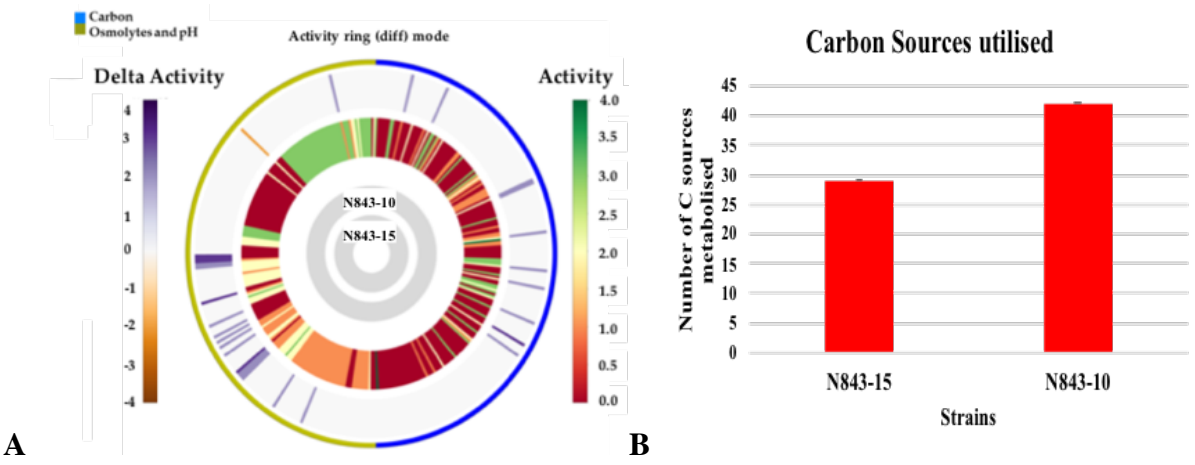

FIG. 7. Comparison of N843-10 and N843-15 metabolic capacity and stress tolerance: **(A)** Metabolic activity ring based on the PM array comparison of N843-15 and N843-10 with respect to carbon source utilization (PM01 and PM02) and stress (osmolytes and pH; PM09 and PM10) resistance: gray inner circles indicate the strains' order; external circle indicates the PM categories. (i) The activity index (AV) calculated for each strain and well is reported as color stripes going from red (AV = 0) to green (AV = 4). (ii) Delta activity: the difference with the AV value of the reference strain is reported when equal to or higher than 2 AV; gray is no difference; purple indicates a higher activity; orange color indicates a lower activity. **(B)** N843-15 utilized 29 whilst N843-10 utilized 42 of the 190 tested carbon sources.

TABLE. 3. Comparison of carbon source utilization ability, pH and osmotic stress tolerance

Intracellular relevant carbon sources	**N843-15**	**N843-10**	**Food relevant carbon sources**	**N843-15**	**N843-10**
Glycerol	-	+	Pectin	-	+
D-Maltose	-	+	D-Arabinose	-	+
D-Cellobiose	-	+	Palatinose	-	+
2-Deoxy-D-Ribose	-	+	D-Tagatose	-	+
Thymidine	-	+	**Osmotic and pH stress**		
Adenosine	-	+	Sodium chloride	-	+
Inosine	-	+	Sodium lactate	-	+
Others			Sodium benzoate at pH 5.2	-	+
3-*O*-Methyl-D-Glucose	-	+	Sodium Nitrite	-	+
5-Keto-D-Gluconic Acid	-	+	β-Phenylethylamine at pH 9.5	+	-

Symbols: **-**, negative reaction; **+**, positive reaction. Opm generated results showing phenotypic variability on different carbon sources as well as under different pH and osmotic stress conditions among the two isolates with N843-10 utilizing the most carbon sources and showing the highest metabolic activities under pH and osmotic stress conditions.

Comparison of N843-10 and N843-15 genomes: We hypothesized that some of the phenotypic differences between N843-10 and N843-15 could be genetically linked. To examine this, we determined and compared whole genome sequences (WGS) in the two strains. *In silico* PCR serotyping and MLST based on the WGS generated from the two strains showed that both N843-10 and N843-10 belonged to PCR serogroup 1/2a, and MLST ST412 and CC412. A WGS based dotblot plot also showed that the genome sequences in the two isolates were co-linear without major chromosomal deletions or re-arrangements (Fig. 8A). Similarly, a phylogenetic tree generated based on the WGS further showed that the N843-10 and N843-15 genomes map to the same phylogenetic branch consistent with the fact that the two strains are clonally identical (Fig. 8B).

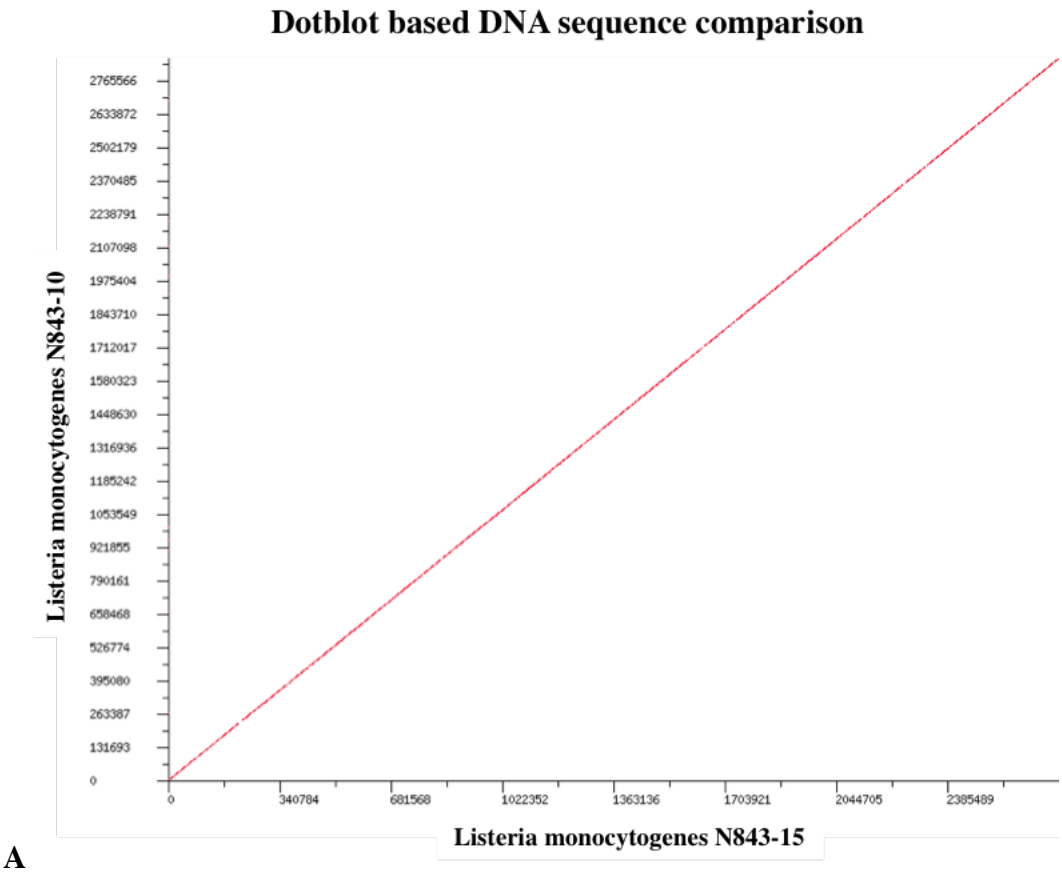

A

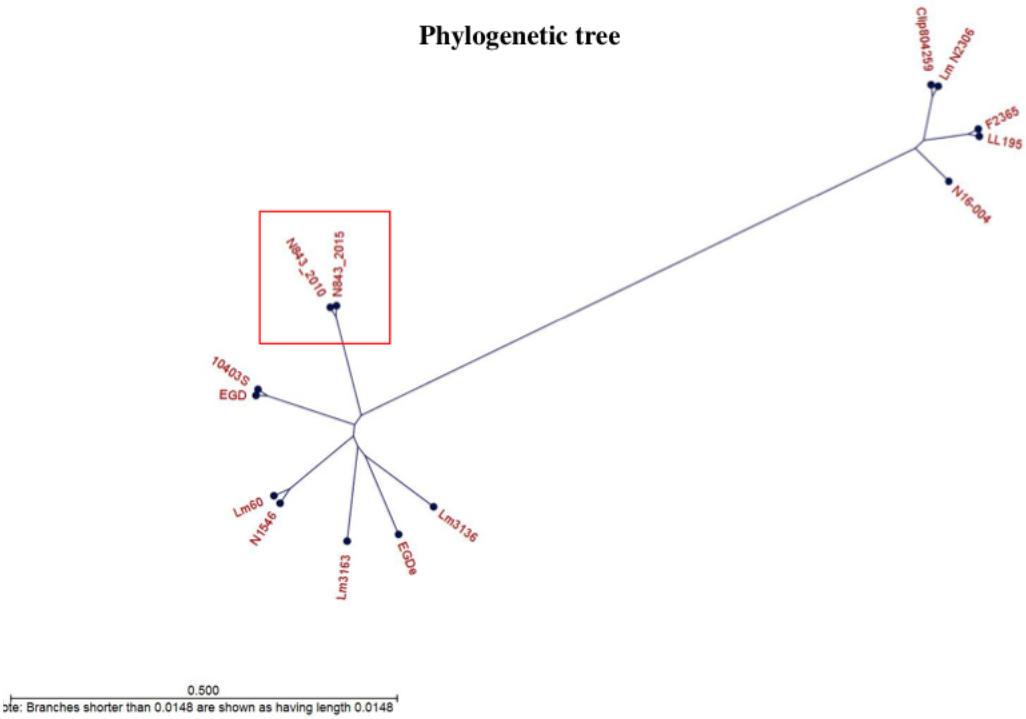

B

FIG. 8. Genome alignment and phylogenetic analysis of the N843-10 and N843-15 isolates: **(A)** Dotblot based DNA sequence alignments between N843-10 and N843-15 genomes showing high genetic conservation. **(B)** WGS based phylogenetic tree showing that N843-15 and N843-10 map to the same phylogenetic branch and therefore derive from the same ancestor.

A comparative analysis of the two genomes detected 26 single nucleotide polymorphisms (SNPs) and 44 insertions and deletion events (InDels) within the N843-15 genome when compared to that of the N843-10 strain (Fig. 8A). Tables 4 and 5 provide an overview of genes and proteins with known functions that were affected through the SNPs and InDels detected in the N843-15 genome relative to that of N843-10. Of the 26 SNPs detected in N843-15, 11 resulted in non-synonymous mutations leading to amino acid changes some of which might therefore have an impact on overall protein function (Table. 4). Among the proteins affected through non-synonymous mutations in N843-15 were the maltose phosphorylase and FIgJ-flagellum specific muraminidase, which are involved in carbohydrate metabolism and flagella assembly functions, respectively. While out of the 44 InDels detected, 21 induced premature stop codons (PMSCs) leading to truncated proteins (Table. 5). There were 12 noteworthy indels leading to PMSC in N843-15 genes that encode proteins with known functions. These included those affecting the genes for the 50S ribosomal protein L15 subunit, a putative galacitol operon regulator, PBDB2, ArcD, HtrA, and RNase J1 of N843-15 (Table. 5). In addition, the WGS analysis in both N843-10 and N843-15 also revealed that the *prfA* gene found in both strains carries a single nucleotide (T) deletion at nucleotide position 680 compared to the *prfA* gene sequence found in the *L. monocytogenes* EGDe strain, which results in a truncated PrfA protein (Fig. 9). It is also important to note that some SNPs and InDels occurred in hypothetical protein coding genes as well as intergenic regions which might have contributed to the observed phenotypes (data not shown).

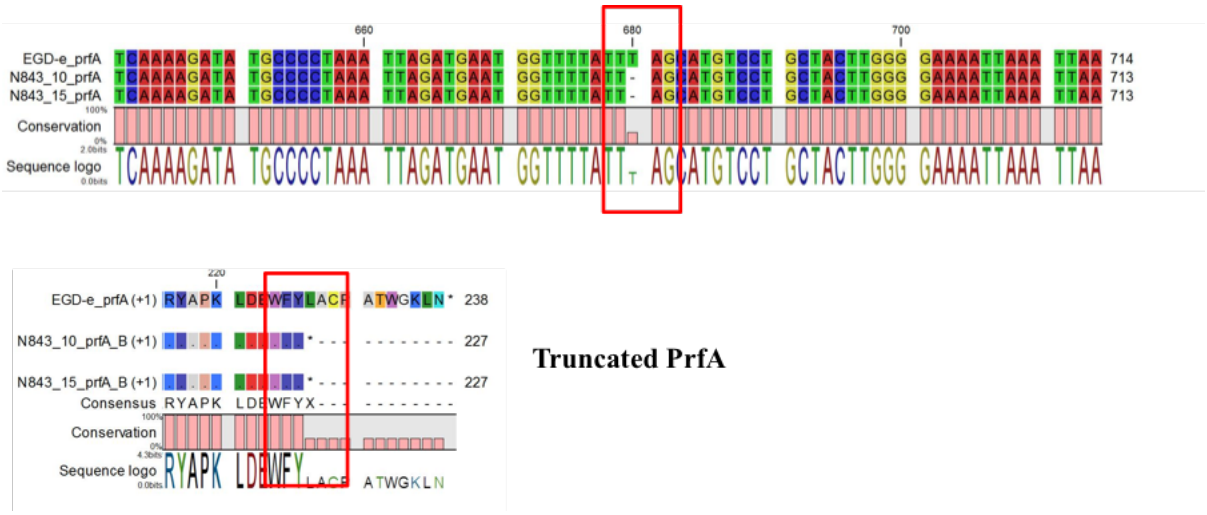

FIG. 9. N843-15 and N843-10 *prfA* genes are identical and carry a single nucleotide deletion leading to truncated PrfA regulator proteins. The red square denotes: (**above**) the regions in the genome of N843-10 and N843-15 were the nucleotide deletion occurred creating a PMSC, (**below**) the consequences in the PrfA protein is truncation by 11 amino acid. The prfA gene nucleotide and amino acid positions are based on *L. monocytogenes* EGDe.

TABLE. 4. Single nucleotide polymorphism detected between N843-15 and N843-10 genomes and their predicted consequences[1]

Gene name[1]	aa change[2]	Side chain class, polarity and charge change	Description of affected protein
lmo0243	A753D	Aliphatic, nonpolar, neutral to acid, acidic polar negative	DNA-dependent RNA polymerase (EC 2.7.7.6)
lmo0972 (dltC)	V7I	Similar	D-alanine-poly (phosphoribitol) ligase subunit 2 (EC 6.1.1.13)
comEC	V25I	Similar	Late competence protein ComEC
lmo1586 (ppnk)	L23S	Aliphatic non-polar neutral to hydroxyl containing polar neutral	NAD kinase (EC2.7.1.23)
lmo2121	I670M	Sulfur containing nonpolar neutral to aliphatic nonpolar neutral	Maltose phosphorylase
lmo2591	V15C	Aliphatic nonpolar neutral to sulfur containing nonpolar neutral	N-acetylmuramoyl-L-alanine amidase (Flg J hydrolase)
lmo2596	P76Q	Cyclic non-polar neutral to amide polar, neutral	30S ribosomal protein
lmo2635	R113S	Basic, basic polar positive to hydroxyl containing polar neutral	1,4-dihydroxy-2-naphthaloate octaprenyltransferase
lmo2829	C194R	Sulfur containing, nonpolar neutral to basic, basic polar, positive	Putative nitroreductase HBN1

[1]Only those SNPs in coding regions are listed. [2]Based on *L. monocytogenes* EGDe genome annotation; [3]Amino acid change.

TABLE. 5. InDels detected in the N843-15 genome compared to N843-10[1]

Gene name[2]	Insertion or deletion	Length in N843-10[3]	Length in N843-15[3]	Description of changes in N843-15[4]
lmo0292	A deletion	501	100	PMSC creating a truncated HtrA protein
23S rRNA	G deletion			Altered 23S rRNA sequence
lmo0533	ATG deletion	89	0	UPF0237 protein- methionine (start codon) lost from coding gene hence no translation
lmo1027	A deletion	556	443	aa change and PMSC leading to truncated Ribonuclease J protein
clpQ	A insertion	179	125	PMSC creating a truncated ATP dependent protease HsIV (E.C.3.4.25-)
potA	CATGAGT	118	306	aa change and loss of stop codon - potA and potB of
potB	deletion	202		a putative ABC transporter fused
lmo1799	584 bp deletion	956	762	Truncated putative peptidoglycan bound protein (LPXTG motif)
hly-III	T-deletion	211	207	PMSC creating truncated hemolysin III protein
16S rRNA	C deletion			16S rRNA
lmo2590	AAA deletion	342	341	Lysine at position 131 deleted in Mrp/Nbp35 family ATP binding protein
rplO	A deletion	146	81	PMSC creating a truncated 50S ribosomal protein L15 subunit
bvrA	T deletion	689	46	L47PMSC creating a truncated predicted regulator of galactitol operon (BglG), (E.C.2.7.1.69) and aa changes N45T and W46G
lmo0842	9 bp insertion	2063	2066	3 aa insertion into putative peptidoglycan bound protein (LPXTG motiff)
pyrG	TTG insertion	553	533	PMSC creating truncated CTP synthase (E.C.6.3.4.2)
rpsE	A-deletion	167	145	PMSC creating truncated SSU ribosomal protein S5p (S2e)
lmo2812	A-insertion	272	258	K259PMSC creating truncated D-alanine carboxypeptidase (PBDB2) and aa changes R257T and F258V.
arcD	G deletion	270	245	PMSC creating truncated Arginine/Ornithine antiport protein

[1]Only those InDels affecting proteins with known functions are listed. [2]Based on *L. monocytogenes* EGDe genome annotation; [3]length as amino acid number. [4]Premature stop codon (PMSC).

Discussion

In this study we describe the comparative analysis of two strains that derived from an identical clone of *L. monocytogenes* but were isolated in 2010 (N843-10) and 2015 (N843-15), respectively, from a persistent human PJI. The PJI involved had a duration of more than 5 years, which represents the longest persistence of a listeriosis infection recorded in literature to date (Kleemann *et al*., 2009). These two strains turned out to be variants derived from the same CC412 *L. monocytogenes* clone but with significant phenotypic differences. Our observations thus suggest that the original *L. monocytogenes* N843-10 strain first isolated in 2010 had either mutated or evolved while resident within the PJI environment giving rise to the second strain *L. monocytogenes* N843-15, which was isolated five years later in 2015. In a previous case from France, three distinguishable *L. monocytogenes* strains that were also derived from a common clone were isolated simultaneously during analysis of the same sample of septic joint fluid but displayed phenotypic differences in hemolysis (Charlier *et al*., 2012).

Our phenotypic analysis revealed that despite being clonally identical, in addition to slower growth and aggregation during growth in broth, the N843-15 strain demonstrated an altered morphology suggestive of incomplete cell division and disrupted cell wall synthesis processes when compared to the parent N843-10 strain, that had been recovered from the same PJI five years prior to N843-15 isolation (Fig. 1, 2, and 3). Moreover, this isolate also showed deficiencies in growth, motility, antibiotic resistance, biofilm forming ability, carbon source utilization, virulence and stress resistance in comparison to the earlier isolate N843-10 (Fig. 1 to 8, Tables 2 and 3). Genome sequence comparison in the two strains allowed identification of various subtle genetic changes that occurred over 5 years of residence in the prosthetic joint capsule environment between the two strains. Notable genetic alterations detected that might potentially explain some for the main phenotypic differences between N843-15 and N843-10 include mutations discovered in the *lmo2812*, *htrA*, *clpQ* and *rnjA* genes of N843-15 (Tables 4 and 5).

Overall the range of phenotypic defects exhibited by N843-15 suggest an acquisition of deficiencies related to nutrient assimilation, cell division and cell wall synthesis during the course of the PJI. Since the cell wall represents an important physical cell barrier modified for protein secretion and large-molecule transport, events key to normal bacterial growth and cell division, the defects observed in the N843-15 cell wall could have disrupted the transportation

of molecules in and out of the cell resulting in the different observed phenotypes (Korsak *et al*., 2010; Allonzo *et al*., 2011).

One of the major genetic changes found in N843-15 is a mutation in the *rnjA* gene leading to a truncation of the RNAse J1 protein. It is interesting to note that some of the morphological phenotypic defects observed in N843-15 such as the disordered peptidoglycan and cell chaining are similar to those described in *Bacillus subtilis* cells depleted of the RNases J1, a protein that is involved in RNA turnover in the bacterial cell (Hunt *et al*., 2006; Figaro *et al*., 2013). Although the phenotypic defects observed in the case of *B. subtilis* were less severe than those observed in N843-15. This might possibly be explained by mutations in other cell wall biosynthesis proteins detected in N843-15 in addition to the RNase J1 truncation mutation (Table. 5).

Penicillin-binding proteins (PBPs) are central in maintaining the uniform shape of bacteria as was seen with PBP-5, a DD-carboxypeptidase, in *E. coli* (Principe *et al*., 2009). Another mutation detected in N843-15 involves the gene encoding for PBPD2 (*lmo2812*). This is a PBP shown to be important for latter stages of peptidoglycan synthesis and cell wall turnover in *L. monocytogenes*. Mutations such as the single nucleotide (A) insertion that generated a PMSC in *lmo2812* creating a truncated D-alanine carboxypeptidase (PBDB2) could further explain the observed altered morphology of N843-15 which at times presented as elongated slightly C-shaped cells. Furthermore, changes involving a 9 bp insertion and a 584 bp deletions to the *lmo0842* and *lmo1799* genes respectively in N843-15 could also have contributed to the altered morphological attributes in this strain compared to the N843-10 parent strain.

Bacterial survival in the outside environment depends on the synthesis and assembly of bacterial flagella in addition to the regulated secretion of proteins and factors that aid in nutrient acquisition (Desvaux and Hebraud, 2006; Toledo-Arana *et al*., 2009; Alonzo *et al*., 2011). N843-15 was less motile than N843-10 (Fig. 1D), most likely due to its filamentation and disordered cell wall structure. As such the chained incompletely separated N843-15 cells might either be too large to move, or they do not provide anchorage for flagella assembly due to the disordered cell wall. In addition, N843-15 also carries a SNP that leads to an amino acid change in the protein Flg J compared to N843-10. Flg J is a flagellum specific muraminidase that is involved in flagella assembly. It is possible that the detected amino acid change in N843-15 might lead to improper flagella assembly and hence contribute to reduced motility in this strain. Such a hypothesis needs to be experimentally confirmed in future studies.

The loss of motility shown on the other hand might represent a deliberate change linked to bacterial adaptation to a specific host environment as was seen previously with *L. monocytogenes* that it down regulates expression of motility related genes when inside the host (Toledo-Arana *et al*., 2009). It is thus plausible that changes leading to reduction of motility in N843-15 might be linked to adaptation in this strain to the PJI environment.

We also observed that co-culturing N843-15 with N843-10 significantly reduces the N843-15 aggregation during growth in BHI broth (Fig. 4). This could be due to the N843-10 parent strain supplementing a substance or enzyme that is lacking in N843-15. However, since adding the supernatant from N843-10 strain cultures failed to accomplish the same effect we concluded that the substance or substances released from N843-10 during growth have a very short half-life. Alternatively, the lack of N843-15 aggregation when co-cultured with N843-10 could also have been an effect of nutrient competition when the two strains are co-cultured**.** Further experiments in future including the microscopic examination during the co-culture experiments would be necessary to show if the cell morphology defects in N843-15 were truly diminished when co-cultured with N843-10**.**

A comparison of antibiotic resistance revealed that N843-15 is more sensitive to a wide range of antibiotics compared to the parent strain N843-10 (Table. 2). The peptidoglycan is the main stress-bearing constituent of the bacterial cell wall, which gives the cell its rigidity and structure, averts osmotic lysis, resists toxins, and is also the target for many antibiotics (Principe *et al*., 2009; Alonzo *et al*., 2011). The observed alterations in genes involved in cell wall biosynthesis and cell wall structure (Table. 5), give a possible reason for the increased sensitivity to cell wall targeting antibiotics. As shown by electron microscopy the peptidoglycan layer in N843-15 is thin and highly disordered (Fig. 3). One consequence of this might be increased permeability to various antibiotics in this strain compared to N843-10. A PMSC detected in the 50S ribosomal protein L15 subunit coding gene of N843-15, a protein involved in translation might also explain why this strain demonstrated an increased sensitivity to 50S subunit (e.g tetracycline and azithromycin) but not 30S subunit (e.g gentamicin) targeting antibiotics. N843-15 which also carries a mutation leading to truncated HtrA is more sensitive to Penicillin G compared to N843-10. This observation is in agreement with previous work that demonstrated that *L. monocytogenes htrA* mutants are hypersensitive to Penicillin G (Stack *et al*., 2005). As already mentioned above N843-15 also carries an RNAse J1 mutation

leading to protein truncation. RNase J1 mutants in *Bacillus subtilis* have also been found to have an increased sensitivity to various antibiotics (Firago *et al*., 2013).

Though, N843-15 was more sensitive to most of the tested antimicrobials in comparison to the wild type, it was less sensitive to the dihydropteroate synthetase inhibitor sulfamethoxazole, similar to observations by (Hunt *et al*., 2006) on RNase J1-depleted *B. subtilis* cells. It would be prudent to investigate the reason for this behavior in the future as we are not clear why the mutant is slightly more resistant to this antibiotic. Overall, both N843-10 and N843-15 are considered sensitive to the tested antibiotics using the CSLI standards including those used for treatment. It is therefore highly unlikely that the N843-15 might have emerged and persisted during the PJI course following a mutation in the parent strain N843-10, which conferred increased resistance leading to selection in presence of some of the different antibiotics used in the PJI patient. It can however not be ruled out that both N843 strains could have survived antibiotic therapy due to failure to achieve bactericidal antibiotic levels in the prosthetic joints for sufficient time because of poor perfusion and or short antibiosis duration.

PJI pathogenesis varies from that of a native joint since these infections rely on biofilm formation and *L. monocytogenes* has a high affinity for implants (Bader *et al*., 2016; Francolini and Donelli, 2010). Biofilm environments protects the bacterium from exposure to antibiotics and possibly the immune system (Kleemann *et al*., 2009). Although it remains possible that N843-15 could have persisted as a biofilm in the PJI our analysis here showed that this strain forms less biofilm compared to the N843-10 parent strain. Reduced biofilm formation in N843-15 can in part be explained by the fact that this strain carries a single nucleotide deletion inducing an HtrA truncation, and *L. monocytogenes htrA* null mutants were found to have a decrease biofilm forming ability (Wilson *et al*., 2006). Our results suggested that it is unlikely that N843-15 could have emerged and survived over time in the PJI due to enhanced biofilm production compared to N843-10. It is however important to also note that our biofilm assays were conducted under laboratory conditions using attachment surfaces differ from those encountered within the human prosthetic joint, which might have favored more biofilm formation by N843-15.

As an intracellular pathogen, *L. monocytogenes* adheres to and invades host cells, then replicates within the cytosol, and individual bacteria are propelled into neighboring cells to spread within host tissues causing different disease outcomes (Pilgrim *et al*., 2003; Chatterjee

et al., 2006; Scharer *et al*., 2013; Radoshevich and Cossart, 2018). Its virulence and survival within host cells is dependent on a variety of secreted virulence proteins such as listeriolysin O (LLO) and cell surface expressed internalins, which are mainly transcriptionally regulated through the transcription regulator PrfA (Chatterjee *et al*., 2006; Desvaux and Hebraud, 2006; Cossart and Lebreton, 2014; Radoshevich and Cossart, 2018). Based on the clinical data of this persistent PJI case, it seems the N843 strains persisted in the joint without much deleterious health effects on the host, which suggests low virulence on the part of the bacterium. Consistent with this notion, low virulence capacity was detected in both N843-10 and N843-15 strains based on the different virulence assays we applied in this study.

Both strains showed reduced LLO secretion as evidenced by their lower hemolysis, as well as diminished epithelial cell invasion abilities when compared to the *L. monocytogenes* LL195 strain used as a reference (Fig. 6). Moreover, both strains were not virulent when examined in the zebrafish embryo-based infection model. Between the two N843 strains, the cell invasion capacity of N843-15 was however significantly lower than that of N843-10. We hypothesize that this might probably be due to its filamentous morphology and/or disordered cell wall, which might have caused improper display or anchoring of cell surface associated virulence factors such as the internalins. More importantly, however, both N843-10 and N843-15 carry an identical single nucleotide deletion in the *prfA* gene that leads to a PrfA protein with a truncated dimerization domain (Fig 9). Since PrfA dimerization is needed for DNA binding the truncated protein in the N843 strains cannot efficiently dimerize and bind to the PrfA box resulting in impaired expression of various virulence genes including those encoding for the hemolysin LLO and internalins A and B (de las Heras *et al*., 2011; Cossart and Lebreton, 2014; Radoshevich and Cossart, 2018). This genetic defect thus also explains the relatively low hemolysis, cell invasion and zebrafish virulence exhibited in both N843 strains when compared to strains harboring intact PrfA proteins such as LL195 and N12-1273.

LLO is important for intracellular survival through facilitating escape from oxidative damage within the phagocytic vacuole and altering host cell gene expression through processes such as histone modifications (Chatterjee *et al*., 2006; Schärer *et al*., 2013; Cossart and Lebreton, 2014; Radoshevich and Cossart, 2018). The non-hemolytic nature of our isolates (Fig. 6), could insinuate that the variants survived extracellularly during their residency in the prosthetic joint. A non-hemolytic phenotype was also observed in a previous case were one of the *L. monocytogenes* isolates from a PJI was also non-hemolytic (Charlier *et al*., 2012). Our findings

therefore provide further evidence in support of the notion that prosthetic joint environments give a sanctuary in which pathogens such as *L. monocytogenes* can persist relatively unexposed to immune defenses (Charlier *et al*., 2012).

Our comparison of the two strains on phenotypic microarrays revealed losses in the ability to utilize various carbon sources and stress resistance phenotypes overtime in the N843 clone during transition from N843-10 to N843-15 (Fig. 7, Table. 3). Notably, N843-15 showed reduced metabolic rate and negative phenotype responses on various intracellular and food relevant carbon sources such as glycerol and pectin, respectively, as well as in presence of stressors such as sodium chloride, sodium lactate and sodium benzoate. Based on these observations we presume that sacrificing some of these phenotypic abilities might be associated with N843-15 evolving to adapt to the human host prosthetic joint capsule environment by switching off some genes that are not necessary in the new environment. At genome level observed differences in carbon source utilization ability could have been due to SNP induced amino acid changes and PMSC inducing InDels detected in proteins that are involved in carbon metabolism such as maltose phosphorylase (loss of D-maltose utilization ability), D-alanine ligase, and the predicted BglG anti-terminator of the galactitol operon, BvrA. It is tempting to speculate that the loss of N843-15 ability to utilize glycerol, one of the main intracellular carbon sources, could have been due to this strain's adaptation to its residence in extracellular environment of the joint fluid where this function is not needed.

Meanwhile alterations in the peptidoglycan structure, as well as the protein truncating *clpQ*, *arcD* and *htrA* gene mutations acquired by N843-15 could all contribute to the observed slower metabolic rate under low pH and increased sensitivity towards osmotic stress conditions compared to N843-10. *A*djustments in the peptidoglycan architecture promotes survival in diverse environments that include soil and the cytosol of mammalian cells (Alonzo *et al*., 2011). Proteases HtrA and the ClpQ are both involved in *L monocytogenes* general stress responses through degradation of misfolded proteins that accumulate during stress exposure (Stack *et al*., 2005; Bowman *et al*., 2008). Whilst ArcD contributes to acid stress tolerance via the ADI system by facilitating exchange of intracellular ornithine for extracellular arginine in *L. monocytogenes* (Kocaman and Sarımehmetoğlu, 2016). Regardless of the *arcD* mutation, N843-15 did not completely lose its acid stress tolerance, which manifested as reduced metabolic rate under such stress. This is indicative that the acid stress response mechanism in this isolate was still functional albeit less efficient. Although not yet proven, the overall

reduction in ability to utilize intracellular C sources, as well as low acid stress tolerance and hemolytic ability are suggestive of the N843-15 joint isolate being evolved to an extracellular life but within the human prosthetic joint environment.

To cope with osmotic stress, many bacteria have evolved intricate osmoregulatory systems to maintain their osmotic equilibrium. *L monocytogenes* acclimates to osmotic stress by intracellular accumulation of low-molecular-weight organic solutes such as, glutamate, trehalose, glycine–betaine, and poly-amines (Principe *et al*., 2009; Soni *et al*., 2011; Kocaman and Sarımehmetoğlu, 2016). Furthermore, the rigidity of the peptidoglycan structure prevents osmotic lysis. This structure is constantly remodeled by the PBPs, to meet the demands of an ever-changing harsh environment (Principe *et al*., 2009; Alonzo *et al*., 2011; Bergholz *et al*., 2012). Similar to what was observed with DD-carboxypeptidase mutants of *Ochrobactrum species* 11a and *L. monocytogenes* H7858 (Principe *et al*., 2009; Bergholz *et al*., 2012), N843-15 also displayed increased sensitivity to osmotic stress in comparison to the parent strain (Fig 7B). We postulate that the D-alanine carboxypeptidase (PBDB2-*lmo2812*) mutation seen in N843-15 could have contributed to the increased sensitivity to osmotic stress detected.

Genome comparison between N843-10 and N843-15 revealed various SNPs and InDels, some of which might contribute to the various phenotypic differences observed between the two strains as already discussed. It is, however, important to note that going, forward specific gene targeting mutagenesis and complementation approaches will be necessary to validate some of the main observations reported here. Meanwhile the N843-15 genome changes detected relative to the N843-10 parent strain demonstrates vestigiality suggestive of short-term adaptation through inactivation and retainment of the unnecessary genes. In long-term adaptation an eventual complete loss of the unnecessary genes would be expected. The relatively low number of genetic variability between the two strains is consistent with high level genome conservation associated with *L. monocytogenes*. Another likely contribution to the low mutation rate could be that the strains were replicating at a much low rate within the PJI environment. It is important to note that most of the mutations were point mutations. Interestingly the PJI case described in 2008 had acquired a serotype changing point mutation in the *ldh* gene of one of the 3 strains isolated from the same septic joint fluid (Charlier *et al*., 2012). This could be suggestive that the prosthetic joint or native joint environment offers an environment that increases the chance of point mutations.

In conclusion, we have characterized two clonally identical *L. monocytogenes* strains N843-10 and N843-15 that were isolated 5 years apart from a persistent rare manifestation of listeriosis. We show that the long-term residence of this bacterium within a human host PJI environment was associated with a wide range of phenotypic changes altering its virulence, metabolic flexibility and fitness under stress conditions. These phenotypic changes were linked to various genetic changes indicating persistence and short-term evolution of *L. monocytogenes* to life within the PJI environment within the human host. We presume that the genetic and phenotypic differences observed between the N843-10 and N843-15 strains could be associated with *L. monocytogenes* evolution to adapt to the prosthetic joint environment within the human host leading to phenotypic heterogeneity within a natural *L. monocytogenes* population. Overall our observations besides highlighting the phenotypic and genotypic variations between these two strains might provide insights into some of the molecular mechanisms underlying host adaptation and evolution of *L. monocytogenes* within the environment of the human PJI.

References

1. **Allerberger F, and Wagner M**. 2010. Listeriosis: a resurgent foodborne infection. Clin. Microbiol. Infect; 16 (1): 16-23.
2. **Alonzo F, McMullen D.P, and Freitag N.E**. 2011. Actin polymerization drives septation of *Listeria monocytogenes namA* hydrolase mutants, demonstrating host correction of a bacterial defect. Infect. Immun; 79 (4): 1458-1470.
3. **Althaus D, Lehner A, Brisse S, Maury M, Tasara T, and Stephan R**. 2014. Characterization of *Listeria monocytogenes* strains isolated during 2011-2013 from human infections in Switzerland. Foodborne. Pathog. Dis*;* 11: 753-758.
4. **Anonymous.** 2010. Methods for Antimicrobial Dilution and Disk Susceptibility Testing for Infrequently Isolated or Fastidious Bacteria: Approved Guideline-Second edition, Volume 30. Number 18, CLSI M45 A2 document.
5. **Anonymous**. 2017. The European Union summary report on trends and sources of zoonoses, zoonotic agents and food-borne outbreaks in 2016. EFSA Journal; 15 (12): 5077.
6. **Anonymous**. 2018. Centre for disease control and prevention. Preliminary incidence and trends of infections with pathogens transmitted commonly through food. Foodborne Diseases Active Surveillance Network, 10 U.S. Sites, 2006-2017. MMWR Morb. Mortal. Wkly Rep; 67 (11): 324-328.
7. **Bader G, Al-Tarawneh M, and Myers J**. 2016. Review of Prosthetic Joint Infection from *Listeria monocytogenes*. Surg. Infect; 17: 739-744.
8. **Bergholz T.M, Bowen B, Wiedmann M, and Boor K.J**. 2012. *Listeria monocytogenes*shows temperature-dependent and -independent responses to salt stress, including responses that induce cross-protection against other stresses. Appl. Environ. Microbiol; 78: 2602–2612.
9. **Bille J**. 1990. Epidemiology of human listeriosis in Europe with special reference to the Swiss outbreak, p 71-74 In Miller AJ, Smith JL, Somkuti GA, editors. Foodborne listeriosis. Elsevier, New York.
10. **Bowman J.P, Bittencourt C.R, and Ross T**. 2008. Differential gene expression of *Listeria monocytogenes* during high hydrostatic pressure processing. Microbiol; 154: 462–475.
11. **Bush L.M, Alrifai A, and Perez M.T**. 2015. *Listeria monocytogenes* prosthetic joint infections a review a propos a case report. Infect. Dis. Clin. Pract; 23: 66-69.

12. **Charlier C, Leclercq A, Cazenave B, Desplaces N, Travier L, Cantinelli T, Lortholary O, Goulet V, Le Monnier A, and Lecuit M**. 2012. *Listeria monocytogenes* – associated joint and bone infections: a study of 43 consecutive cases. Clin. Infect. Dis; 54: 240-248.
13. **Chatterjee S.S, Hossain H, Otten S, Kuenne C, Kuchmina K, Machata S, Domann E, Chakraborty T, and Hain T**. 2006. Intracellular gene expression profile of *Listeria monocytogenes*. Infect. Immun; 74: 1323-1338.
14. **Chavada R, Keighley C, Quadri S, Asghari R, Hofmeyr A, and Foo H.** 2014. Uncommon manifestations of *Listeria monocytogenes* infection. BMC Infect. Dis: 14: 641.
15. **Chougle A and Narayanaswamy V**. 2004. Delayed presentation of prosthetic joint infection due to *Listeria monocytogenes*. Int. J. Clin. Pract; 58: 420-421.
16. **Cone L.A, Fitzmorris A.O, Hirschberg J.M**. 2001. Is *Listeria monocytogenes* an important pathogen for prosthetic joints? J Clin Rheumatol; 7:34-37.
17. **Cossart P and Lebreton A**. 2014. A trip in the ''New Microbiology'' with the bacterial pathogen Listeria monocytogenes. FEBS Letters; 588: 2437–2445.
18. **Darling** AE, Mau B, Perna NT. 2010. ProgressiveMauve: multiple genome alignment with gene gain, loss and rearrangement. PLoS One; 5 (6): e11147.
19. **de las Heras A, Cain R.J, Bielecka M.K, and Vázquez-Boland J.A**. 2011. Regulation of Listeria virulence: PrfA master and commander. Curr. Opin. Microbiol; 14: 118-27.
20. **Del Pozo J, Garcia de la Garza R, Diaz de Rada P, *et al***. 2013. *Listeria monocytogenes* septic arthritis in a patient treated with mycophenolate mofetil for polyarteritis nodosa : a case report and review of the literature. Int J Infect Dis; 17: 132-133.
21. **Desvaux M, and Hebraud M**. 2006. The protein secretion systems in Listeria: inside out bacterial virulence. FEMS Microbiol. Rev; 30: 774–805.
22. **Ebner R, Stephan R, Althaus D, Brisse S, Maury M, and Tasara T**. 2015. Phenotypic and genotypic characteristics of *Listeria monocytogenes* strains isolated during 2011-2014 from different food matrices in Switzerland. Food Control; 57: 321-326.
23. **Eshwar A.K, Guldimann C, Oevermann A and Tasara T**. 2017. Cold-shock domain family proteins (Csps) are involved in regulation of virulence, cellular aggregation, and

flagella-based motility in *Listeria monocytogenes*. Front. Cell. Infect. Microbiol; 7: 453.

24. **Figaro S, Durand S, Gilet L, Cayet N, Sachse M, and Condon C.** 2013. *Bacillus subtilis* mutants with knockouts of the genes encoding Ribonucleases RNase Y and RNase J1 are viable, with major defects in cell morphology, sporulation, and competence. J. Bacteriol; 195: 2340-2348.
25. **Francolini I and Donelli G**. 2010. Prevention and control of biofilm-based medical-device-related infections. FEMS Immunol. Med. Microbiol; 59:227-38.
26. **Galardini M, Mengoni A, Biondi E.G, Semeraro R, Florio A, Bazzicalupo M, Benedetti A, and Mocali S**. 2014. DuctApe: a suite for the analysis and correlation of genomic and OmniLog™ phenotype microarray data. Genomics; 103: 1-10.
27. **Glaser P, Frangeul L, Buchrieser C, Rusniok C, Amend A, Baquero F, *et al***. 2001. Comparative genomics of Listeria species. Science; 294: 849-852.
28. **Göker M, Hofner B, Montero Calasanz M.d.C, Sikorski J, and Vaas L.A.I**. 2016. opm: An R package for analysing phenotype microarray and growth curve data. Phenotype Microarray Data: 1-68.
29. **Guldimann C, Bärtschi1 M, Frey J, Zurbriggen A, Seuberlich T, and Oevermann A**. 2015. Increased spread and replication efficiency of *Listeria monocytogenes* in organotypic brain-slices is related to multilocus variable number of tandem repeat analysis (MLVA) complex. BMC Microbiol; 15: 134.
30. **Hunt A, Rawlins J.P, Thomaides H.B, and Errington J.** 2006. Functional analysis of 11 putative essential genes in *Bacillus subtilis*. Microbiol; 152: 2895-2907.
31. **Jolley K.A. and Maiden M.C.J**. 2010. BIGSdb: scalable analysis of bacterial genome variation at the population level. BMC Bioinformatics; 11: 595.
32. **Kocaman N and Sarımehmetoğlu B**. 2016. Stress Responses of *Listeria monocytogenes*. Ankara Üniv. Vet. Fak. Derg; 63: 421-427.
33. **Kesteman T, Yombi J.C, Gigi J, *et al***. 2007. Listeria infections associated with infliximab: case reports. Clin. Rheumatol; 26: 2173-2175.
34. **Kleemann P, Domann E, Chakraborty T, Bernstein I, and Lohoff M**. 2009. Chronic prosthetic joint infection caused by *Listeria monocytogenes*. J. Med. Microbiol; 58: 138-141.

35. **Korsak D, Markiewicz Z, Gutkind G.O, and Ayala J.A**. 2010. Identification of the full set of *Listeria monocytogenes* penicillin-binding proteins and characterization of PBPD2 (Lmo2812). BMC Microbiol; 10:239.
36. **Krumsiek J, Arnold R, Rattei** T. 2007. Gepard: a rapid and sensitive tool for creating dotplots on genome scale. Bioinformatics; 23 (8): 1026-8.
37. **Moura A, Criscuolo A, Pouseele H, Maury MM, Leclercq A, Tarr C, *et al*.** 2016. Whole genome-based population biology and epidemiological surveillance of *Listeria monocytogenes*. Nat. Microbiol; 2:16185.
38. **Pilgrim S, Kolb-Maurer A, Gentschev I, Goebel W, and Kuhn M**. 2003. Deletion of the gene encoding p60 in *Listeria monocytogenes* leads to abnormal cell division and loss of actin-based motility. Infect. Immun; 71: 3473–3484.
39. **Principe A, Jofre E, Alvarez F, and Mori G**. 2009. Role of a serine-type D-alanyl-D-alanine carboxypeptidase on the survival of *Ochrobactrum sp. 11a* under ionic and hyperosmotic stress. FEMS Microbiol. Lett; 295: 261– 273.
40. **Radoshevich L and Cossart P**. 2018. *Listeria monocytogenes*: towards a complete picture of its physiology and pathogenesis. Nat. Rev. Microbiol; 16: 32–46.
41. **Scharer K, Stephan R, and Tasara T.** 2013. Cold shock proteins contribute to the regulation of listeriolysin O production in *Listeria monocytogenes*. Foodborne Path. Dis; 10: 1023-1029.
42. **Shuman E.K, Urquhart A, and Malani P.N**. 2012. Management and prevention of prosthetic joint infection. Infect. Dis. Clin. North Am. 26 (1): 29–39.
43. **Soni K.A, Nannapaneni R, and Tasara T**. 2011. *An overview of stress response proteomes in Listeria monocytogenes*. Agric. Food Anal. Bacteriol; 1 (1): 66-85.
44. **Stessl B, Rückerl I, and Wagner M**. 2014. Multilocus Sequence Typing (MLST) of *Listeria monocytogenes*. In: Jordan K., Fox E., Wagner M. (eds) *Listeria monocytogenes*. Methods in Molecular Biology (Methods and Protocols), Volume 1157. Humana Press, New York, NY.
45. **Toledo-Arana A, Dussurget O, Nikitas G, Nina Sesto N, Guet-Revillet H, Balestrino D, *et al*.** 2009. The Listeria transcriptional landscape from saprophytism to virulence. Nature; 459: 950–956.
46. **Wilson R.L, Brown L.L, Kirkwood-Watts D, Warren T.K, Lund S.A, King D.S, Jones K.F, and Hruby D.E**. 2006. *Listeria monocytogenes* 10403S HtrA is necessary for resistance to cellular stress and virulence. Infect. Immun; 74: 765-768.

Acknowledgements

Firstly, I would like to thank Prof. Dr. Dr. h.c. Roger Stephan and PD Dr. Taurai Tasara for the opportunity to do my doctoral thesis at the Institute for Food Safety and Hygiene (ILS) University of Zurich and for their invaluable support throughout my thesis. Similarly, I would like to thank the ILS laboratory team who assisted me in the pursuit of achieving this thesis, special mention to PD Dr. Sophia Johler, Dr. Claudia Guldimann, Dr Marc J.A Stevens and Dr. Athmanya Eshwar for their assistance in the translation of the abstract from English to German, cell culture, data analysis and zebrafish experimental work, respectively. Furthermore, I would like to extend my gratitude to the group of Dr. Ueli von Ah at Agroscope Bern and the TEM Unit of the Institute for Veterinary Pathology, Zuerich, (IVPZ) University of Zurich for availing their facilities and all their technical assistance with phenotypic profiling and electron microscopy, respectively. I also thank the team of curators of the Institute Pasteur MLST and whole genome MLST databases for curating the data and making them publicly available at http://bigsdb.pasteur.fr/. Furthermore, I would like to thank Prof. Dr. Franz Allerberger for co-examining my doctoral thesis. Finally, I thank my family and friends, for the support and encouragement. Above all I thank the Almighty God for all things are made possible through Him.

Curriculum Vitae

First name Family name	Francis Muchaamba
Date of birth	27/09/1987
Place of birth	Harare, Zimbabwe
Nationality	Zimbabwean
02/2001– 11/2006	Mutare Boys High School, Mutare, Zimbabwe
11/11/2006	Zimbabwe General Certificate of Education at Advanced level
08/2007 – 08/2013	Studies in Veterinary Science, University of Zimbabwe, Faculty of Veterinary Science, Harare, Zimbabwe
26/08/2013	Bachelor of Veterinary science degree, University of Zimbabwe, Faculty of Veterinary Science, Zimbabwe
11/2016 – 06/2018	Preparation of the thesis under the direction of Prof. Dr. Dr. h.c. Roger Stephan and PD Dr. med. vet. Taurai Tasara at the Institute for Food Safety and Hygiene of the Vetsuisse Faculty, University of Zurich Director Prof. Dr. Dr. h.c. Roger Stephan
11/2016 – 06/2018	Doctrate student/Assistant, Institute for Food Safety and Hygiene, Zurich, Switzerland